Res. Org. Geochem. **31**, 15−28 (2015)

Article

Characterization of organic matter and depositional environment of the Jurassic small sedimentary basins exposed in the northwest onshore area of Sri Lanka

Amila Sandaruwan Ratnayake* and Yoshikazu Sampei*, a

(Received March 7, 2015; Accepted June 1, 2015)

Abstract

The Jurassic sediments in two small basins formed on the Precambrian metamorphic terrain of Sri Lanka, which had been located in the eastern Gondwanaland in mid-latitudes of the southern hemisphere, were investigated to make clear the origin of organic matter (OM) and its depositional environment. Total organic carbon (TOC) contents are high (3.05−5.10%) in brown to black color mudstones in the Jurassic Andigama Basin, while the grey color sandy sediments in the Jurassic Tabbowa Basin generally have very low TOC (0.04−0.17%). The Andigama mudstones are thermally immature, and the Tabbowa sediments and relational Miocene Aruwakkalu limestone are moderately matured in the oil generation stage. The sediment samples from the Jurassic Andigama Basin show a large proportion of middle-chain *n*-alkanes (nC$_{21}$-C$_{25}$), enriched C$_{29}$ steranes, high C/N ratios (16.3−37.8), very low total sulfur (TS <0.001%) and higher pristane/phytane ratios (Pr/Ph=2.1−3.0). These results suggest that the sediments were deposited in freshwater swamp under oxic condition. Abundant retene, simonellite, perylene, 1-methylphenanthrene, 1, 7-dimethylphenanthrene and 1, 2, 7-/1, 2, 9-trimethylphenanthrenes in the Andigama mudstones indicate that the OMs were mainly originated from gymnosperm with fungi. On the other hand, the Jurassic sandy sediments in the Tabbowa Basin have predominant nC$_{16}$-C$_{21}$ alkanes with a minor peak of waxy *n*-alkanes (nC$_{29}$, nC$_{31}$, nC$_{33}$), very low TS (<0.001%), abundant C$_{27}$ steranes and higher Ts/(Ts+Tm) [Ts: 17 α(H)-22, 29, 30-trisnorhopane, Tm: 18 α(H)-22, 29, 30-trisnorhopane] triterpane ratios, which suggesting the OMs from algal origin with a significant terrestrial higher plants. The Miocene Aruwakkalu limestone shows very low TOC (0.06%) and algal origin. The sediment samples from the relational Pleistocene Aruwakkalu Red Earth show a high unresolved complex mixture (UCM), and high values of carbon preference index (CPI=4.78) and average chain length (ACL=29.9), which indicate the OM from oxidized and/or biodegraded ancient terrestrial plant.

1. Introduction

Recent exploration/investigations of petroleum deposits in Sri Lanka have identified several offshore sedimentary basins. The basin in the northwestern offshore area of Sri Lanka has recorded thick sedimentary sequences of marine/continent origins, and natural gas deposits were found (Ratnayake et al., 2014). However, researches in sedimentary organic matter in land area are quite few in Sri Lanka, because about 90% of the land is covered with metamorphic terrain, which are high-grade crystalline non-fossiliferous metamorphic rocks of Precambrian age. Only one-tenth of landmass consists of sedimentary rocks of limited ages including the Jurassic, Miocene and Quaternary (Cooray, 1984). Distribution of the Jurassic sediments are regulated in small basins exposed rarely and sporadically in the western land area, and the Miocene sediments are composed mainly of limestone narrowly exposed along the coastline of northwestern Sri Lanka (Fig. 1(a)). These small sedimentary basins are expected to be preserving significant information about the original OM type, since those are not deeply subsided (buried) and OM is not over matured. Therefore, a study of onshore sedimentary rocks of the basins on the northwest margin of Sri Lanka provides important organic geochemical information to understand the type of OM and depositional environments during the Jurassic age in Sri Lanka. In this paper, organic geochemical proxies including C, N, S elemental analysis and gas chromatography-mass spectrometry (GC-MS) are used to evaluate different sedimentary units including the Miocene limestone and Pleistocene Red Earth beds in the northwest of Sri Lanka.

*Department of Geoscience, Graduate School of Science and Engineering, Shimane University, 1060, Nishikawatsu-cho, Matsue 690-8504, Japan

[a] Corresponding author: Yoshikazu Sampei
E-mail: sampei@riko.shimane-u.ac.jp, Tel: +81 852 32 6453, Fax: +81 852 32 6469

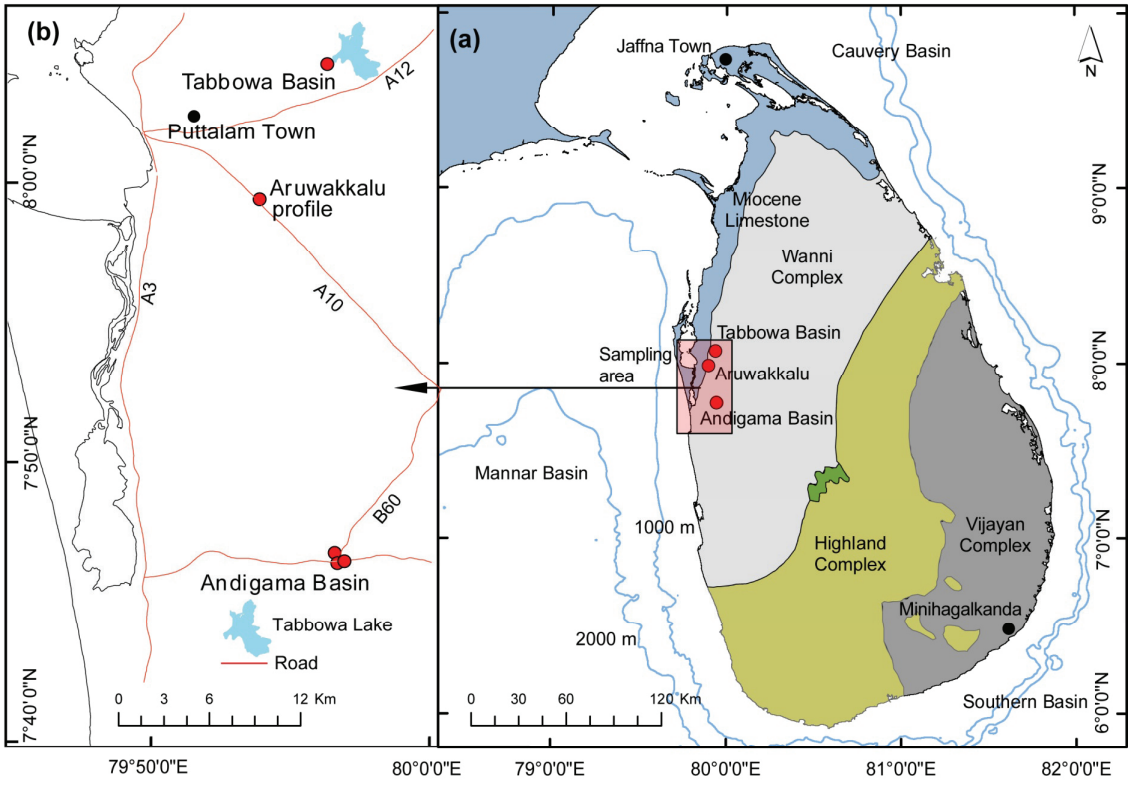

Fig. 1. (a) and (b) A generalized map showing major geological units and sedimentary basins in Sri Lanka (a), and a map showing sample points in the study area (b).

2. Geological background

The Jurassic Gondwana Group sediments occur in Sri Lanka within a few onshore faulted small basins underlain by the Precambrian Wanni Complex (metamorphic rocks) (Fig. 1(a)). The Jurassic sediments can be recognized as one of the oldest unmetamorphosed sedimentary units in the country (Cooray, 1984). The Jurassic sediments are not well exposed in Sri Lanka. These sedimentary beds are much less studied than the Precambrian metamorphic rocks, although several studies have examined their subsurface isostatic gravity anomalies (Tantrigoda and Geekiyanage, 1991) and plant fossil deposition (Edirisooriya and Dharmagunawardhane, 2013). The Jurassic Gondwana sediments examined in the present study were collected in the Andigama and the Tabbowa Basins (Fig. 1(b)). The maximum depths to the basement of the Andigama and Tabbowa Basins are 1.2 and 1.5 km respectively, and a three-dimensional model indicates that approximately 65 km^3 volumes of the Gondwana sediments are deposited in the Andigama Basin (Tantrigoda and Geekiyanage, 1991). In addition, thin coal seams were observed in well cuttings of the Andigama Basin (Cooray, 1984). Although Sri Lanka presently locates about 800 km north of equator (5°N-10°N and 79°E-82°E), it was positioned in the eastern Gondwanaland of mid-latitudes in the southern hemisphere (34°s-37°s and 16°E-21°E) during the Jurassic period. Based on the geological frameworks of Sri Lanka, its separation from the eastern Gondwanaland and its northward motion have been extensively described by several authors (e.g., Molnar and Tapponnier, 1975; Cooray, 1984; Katz, 2000; Chatterjee et al., 2013).

Sri Lanka had moved to the northern hemisphere during the Miocene (4°N-8°N and 77°E-79°E). Several meters thick and widely extended limestone beds were deposited during the Miocene in the northwest (Puttalam-Jaffna) and the southeast (Minihagalkanda) of Sri Lanka (Cooray, 1984) (Figs. 1(a) and (c)). The Pleistocene period of northwest of Sri Lanka is characterized by deposition of thick (about 15–20 m) and elongated Red Earth beds, which are aligned in a north-south direction along the north-west coast (Cooray, 1984) (Fig. 1(c)).

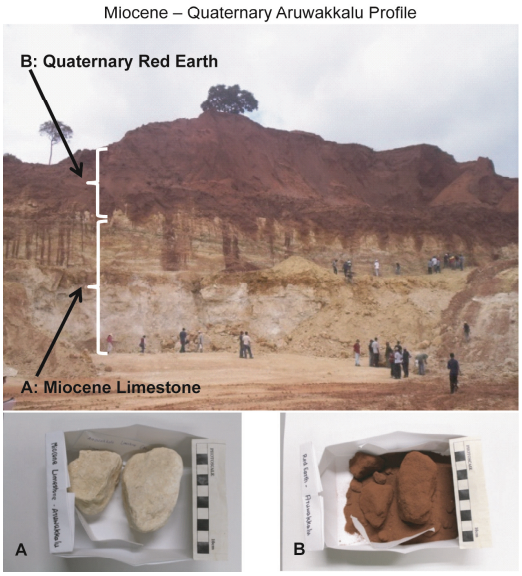

Fig. 1. (c) Field section and samples photographs of the Miocene – Quaternary Aruwakkalu beds.

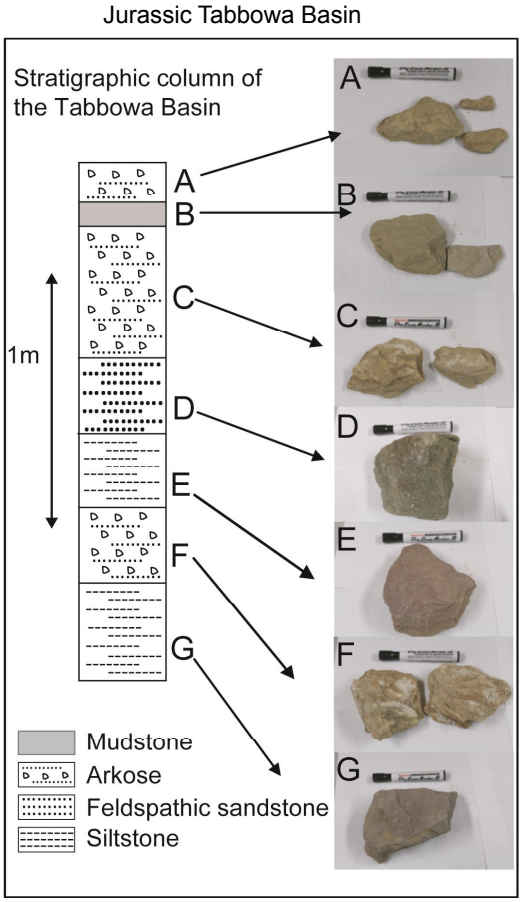

Fig. 1. (e) Stratigraphic successions of the Jurassic Tabbowa Basin.

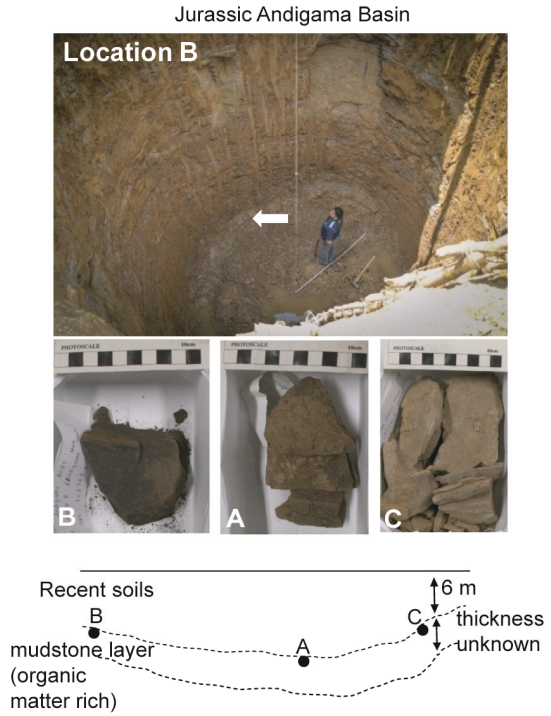

Fig. 1. (d) Field section, samples photographs and simplified structure of the Jurassic Andigama Basin.

3. Samples and analytical methods

The Andigama beds are completely covered with over 5 m thick recent soils (Fig. 1(d)). Four unweathered hard Andigama mudstone samples (three mudstones and one sandy mudstone) were collected from wells sections (7° 46' N and 79° 56' E, 50 m above sea level; Fig. 1(d)). The best exposures of the Jurassic rocks in the Tabbowa Basin were found close to the Tabbowa irrigation tank (8° 04' N and 79° 55' E, 20 m above sea level; Fig. 1(b)). However, the outcrops have been significantly weathered due to fluvial activities in the area. Therefore, outer parts of the samples (about 10 – 20 cm) were carefully removed to separate weathered surface. Seven samples were collected from the Tabbowa beds (Fig. 1(e)) that contain siltstone, arkose sandstone and mudstones (Table 1). In addition, representative samples of the Miocene limestone and the Pleistocene Red Earth were collected from the sedimentary beds at Aruwakkalu (7° 59' N and 79° 54' E, 40 m above sea level; Fig. 1(c)).

Pulverized rock samples were acidified with 1 M HCl to remove carbonate carbon. These samples were then dried on a hotplate at 110ºC for 1 hour. Total organic carbon (TOC), total nitrogen (TN) and total sulfur (TS) percentages were determined on these dried samples using combustion method with a FISONS EA1180

elemental analyzer. Total carbon (TC) contents were determined in the separate run with the FISONS EA1180 elemental analyzer without HCl treatment. Carbonate carbon (carb-C) percentages were calculated based on the difference between TC and TOC contents. BBOT [2, 5-bis-(5-tert-butyl-2-benzoxazol-2-yl)-thiophene] standard was used for the elemental analysis. The authors quantified TOC, TC, TN, TS by correlation to the calibration curve with 5 points regression analysis of the standard.

Bitumen was extracted from the sediments using the soxhlet extraction technique, refluxing for 72 hours using dichloromethane and methanol (9/1, v/v) solvent at 60 ºC. The extracts were condensed in a rotary evaporator and dissolved in hexane. The extractable OM was separated using a thin layer chromatography (TLC) plate (silica gel 60 PF_{254} containing gypsum) with hexane as a mobile phase. The fractions of aliphatic hydrocarbons and polycyclic aromatic hydrocarbons (PAHs) were identified on the TLC plate using UV light. The extracted OMs with hexane from the TLC silica gel was condensed to 100 microliters, and 1 microliter of the liquid was injected to gas chromatograph (GC: Shimadzu 2010) coupled with a mass spectrometer (MS: Shimadzu GC-MS QP2010). The GC is equipped with a programmable temperature injection system and a fused silica capillary column (30 m x 0.25 mm DB 5MS). The temperature was programmed from 50°C to 300°C at the rate of 8°C/min and held at 300°C for 30 minutes with pure helium as a carrier gas. The MS was scanned every 0.5 seconds over *m/z* 50 to 850, and the spectral data obtained were stored in a computer system. All spectra were recorded at an electric energy of 70 eV. The *n*C_{24} tetracosane, cholestane and PAHs mix (Accu Standard Inc. Z-013–17) were used as the external standards.

4. Results

4.1. Bulk measurements

The TC, TOC, TN and TS data are shown in Table 2. The brown to black color mudstone of the Andigama Basin contain abundant OM (TOC; A=3.05, B=5.10 and B2=3.34%). However, the TOC value of sandy brown mudstone is low (0.49%), showing poor OM content in this basin. The Tabbowa beds have very low TOC values ranging from 0.04% to 0.17%. Also, the constancy is evident in the different lithological units (Fig. 1(e)). The Aruwakkalu limestone (Carb-C=10.36%: Table 2) and the Red Earth represent low TOC values of 0.06% and 0.41% respectively. The TN values in all analyzed samples are ranging from 0.01% to 0.20%. The TS values are less than detection limit (<0.001%) in all samples of these basins.

4.2. Molecular compositions

The *n*-alkane data are summarized in Table 3. The *n*-alkanes distribution is characterized by a unimodal pattern with the middle-chain predominance in the Andigama and Aruwakkalu limestone samples, and the short-chain predominance in the Tabbowa and Aruwakkalu Red Earth samples (Fig. 2). The *n*-alkane distributions of the Andigama samples are characterized by an odd predominance at higher molecular weight greater than C_{23} (Fig. 2). Distributions of representative steranes (*m/z*=217) and pentacyclic triterpanes (*m/z*=191) are shown in Fig. 3. A variety of aromatic compounds is present only in brown to black color mudstones of the Andigama Basin (Fig. 4; Table 4). Phenanthrene (P, *m/z*=178), fluoranthene (Fla, *m/z*=202), pyrene (Py, *m/z*=202), benzo[a] anthracene (BaAn, *m/z*=228), chrysene/triphenylene (Chry+Tpn, *m/z*=228), benzofluoranthene (Bflas, *m/z*=252), benzo[e]pyrene (BePy, *m/z*=252), benzo[a] pyrene (BaPy, *m/z*=252), perylene (Pery, *m/z*=252), indeno[cd]pyrene (InPy, *m/z*=276) and benzo[ghi] perylene (BghiP, *m/z*=276) were detected as non-alkylated PAHs. Relative proportions of PAHs of the mudstones in the Andigama Basin are shown in Fig. 5. Cadalene (Cad, *m/z*=183), methylphenanthrenes (MP, *m/z*=192), dimethylphenanthrenes (DMP, *m/z*=206) and trimethylphenanthrenes (TMP, *m/z*=220), simonellite (Sim, *m/z*=237) and retene (Ret, *m/z*=219) were abundant alkylated PAHs in the Andigama mudstones (Figs. 4 and 6).

5. Discussion

5.1. Thermal maturity

The 20S/(20S+20R) ratio of the C_{29} 5α (H), 14α (H), 17α (H)-sterane is one of the most reliable maturity indicator because of a minor influence by source variability. This ratio indicates the oil generative window from the value of 0.25 (Farrimond et al., 1998) and the equilibrium value of 0.52–0.55 (Waseda and Nishita, 1998; Farhaduzzaman et al., 2012). The 22S/(22S+22R) ratio in the C_{31} to C_{35} 17α hopanes is also an important maturity indicator. However, the 22S/(22S+22R) ratios of C_{31} hopanes are often affected by co-elution of a C_{30} neohopane generated during biodegradation (Subroto et al., 1991) and release of sulfurized hopanoids from kerogen (Köster et al., 1997). The hopane 22S/(22S+22R) ratio is more sensitive in lower maturity stage than the sterane 20S/(20S+20R) ratio, and the hopane ratio has the equilibrium value of about 0.6 (Farrimond et al., 1998; Sawada, 2006; Pan et al., 2008). Figure 7 for the cross plots of C_{31} hopanes 22S/(22S+22R) ratios (0.46–0.62) to C_{29} sterane 20S/(20S+20R) ratios (0.15–0.56) shows good

Table 1. Lithological characteristics of the sediments from northwest onshore sedimentary units in Sri Lanka.

Sample	Description of lithological properties	Age
Andigama Basin		
Mudstone A	Brown to black color hard and dense mudstone with black carbonaceous matter	Jurassic
Mudstone B	Brown to black color hard and dense mudstone with larger black carbonaceous matter (ca. 0.1–1 cm)	Jurassic
Mudstone B2	Brown to black color mudstone with small black carbonaceous matter	Jurassic
Sandy mudstone C	Brown color silty mudstone with thin sandy bed	Jurassic
Tabbowa Basin		
Upper arkose bed A	Angular to sub-angular grains of quartz and feldspar associated with reddish color hematite	Jurassic
Mudstone bed B	Dark and/or light gray color mudstone in thin bedding plain	Jurassic
Middle arkose bed C	Quartz and feldspar associated with black fine fragments and thin beds	Jurassic
Feldspathic sandstone D	Medium to coarse grained light brown color sandstone.	Jurassic
Upper siltstone E	Brownish to reddish mudstone associated with fine quartz grains.	Jurassic
Lower arkose bed F	Quartz and feldspar associated with black fine fragments and thin beds	Jurassic
Lower siltstone G	Brownish to reddish mudstone associated with fine quartz grains.	Jurassic
Aruwakkalu Profile		
Aruwakkalu limestone	Hard, partly crystalline, compact rock associated with very fine sands and black organic matter	Miocene
Aruwakkalu Red Earth	Small, rounded quartz grains in earthy material composed of clay and iron oxide	Quaternary

Table 2. C, N, S elemental data of the sediment samples. TN; total nitrogen content, TOC; total organic carbon content, Carb-C; carbonate carbon content, TS; total sulfur content.

Sample	TN (%)	TOC (%)	Carb-C (%)	TS (%)	C/N ratio
Andigama Basin					
Mudstone A	0.174	3.05	0.39	<0.001	17.5
Mudstone B	0.135	5.10	1.02	<0.001	37.8
Mudstone B2	0.205	3.34	0.04	<0.001	16.3
Sandy mudstone C	0.166	0.49	0.08	<0.001	2.9
Tabbowa Basin					
Upper arkose bed A	0.010	0.06	0.02	<0.001	5.6
Mudstone bed B	0.013	0.17	0.01	<0.001	13.1
Middle arkose bed C	0.010	0.09	0.01	<0.001	9.5
Feldspathic sandstone D	0.010	0.06	0.00	<0.001	6.3
Upper siltstone E	0.010	0.04	0.06	<0.001	4.3
Lower arkose bed F	0.009	0.08	0.04	<0.001	8.2
Lower siltstone G	0.011	0.05	n.d	<0.001	5.0
Aruwakkalu Profile					
Aruwakkalu limestone	0.072	0.06	10.36	<0.001	0.9
Aruwakkalu Red Earth	0.035	0.41	n.d	<0.001	11.7

Table 3. Biomarker data of the sediment samples. n.d.: not determined. ACL (average chain length) is expressed as following; ACL = [23(nC_{23}) + 25(nC_{25}) + 27(nC_{27}) + 29(nC_{29}) + 31(nC_{31}) + 33(nC_{33})]/(nC_{23} + nC_{25} + nC_{27} + nC_{29} + nC_{31} + nC_{33}), CPI (carbon preference index) is expressed as following; CPI = 1/2[(nC_{25} + nC_{27} + nC_{29} + nC_{31} + nC_{33})/(nC_{24} + nC_{26} + nC_{28} + nC_{30} + nC_{32}) + (nC_{25} + nC_{27} + nC_{29} + nC_{31} + nC_{33})/(nC_{26} + nC_{28} + nC_{30} + nC_{32} + nC_{34})].

Sample	*n*-alkanes			Isoprenoid	Triterpanes		Steranes					
	$nC_{<20}/nC_{all}$	ACL	CPI	Pr/Ph	22S/(22S+22R) for C_{31} hopane	Ts/(Ts+Tm)	20R (%) C_{27}	20R (%) C_{28}	20R (%) C_{29}	$C_{27}/(C_{27}+C_{29})$	$C_{29}/(C_{27}+C_{28}+C_{29})$	C_{29} 20S/(20S+20R)
Andigama Basin												
Mudstone A	0.21	26.9	1.85	3.0	0.46	0.11	21	11	68	0.24	0.68	0.18
Mudstone B	0.19	27.0	1.93	2.1	0.48	0.07	20	11	70	0.22	0.70	0.17
Mudstone B2	0.23	26.3	1.77	2.7	0.47	0.14	25	13	61	0.29	0.61	0.18
Sandy mudstone C	0.03	26.4	1.86	n.d.	0.47	0.23	25	15	60	0.29	0.60	0.15
Tabbowa Basin												
Upper arkose bed A	0.39	26.5	2.15	0.2	0.53	0.41	38	16	46	0.45	0.46	0.32
Mudstone bed B	0.35	26.9	2.11	0.3	0.50	0.31	27	17	56	0.32	0.56	0.26
Middle arkose bed C	0.61	27.3	2.57	0.7	0.56	0.50	63	12	25	0.72	0.25	0.41
Feldspathic sandstone D	0.53	26.2	2.40	0.4	0.55	0.52	38	26	36	0.52	0.36	0.38
Lower arkose bed F	0.66	25.9	2.25	0.4	0.55	0.42	40	19	41	0.49	0.41	0.41
Lower siltstone G	0.35	26.4	3.07	0.2	0.61	0.51	37	23	40	0.49	0.40	0.45
Aruwakkalu Profile												
Aruwakkalu limestone	0.12	26.2	1.61	n.d.	0.54	0.32	34	22	44	0.43	0.44	0.30
Aruwakkalu Red Earth	0.35	29.9	4.78	0.4	0.62	0.70	48	16	36	0.57	0.36	0.56

correlation between them ($Y=0.40X+0.40$, $r=0.949$ and $n=12$). This result indicates that biodegradation and sulfurized hopanoids were low levels. Low content of unresolved complex mixture (UCM; Fig. 2) expect for the Aruwakkalu Red Earth, and very low sulfur contents (Table 2) are consistent with the result in Fig. 7. The Aruwakkalu Red Earth with higher UCM (Fig. 2) has uncommonly high ratio of C_{31} hopanes 22S/(22S+22R) (Fig. 7). Thus, all Andigama samples are thermally immature, and the Tabbowa and Aruwakkalu sediments are moderately matured in the oil generation main stage (Fig. 7). Moreover, these facts suggest that the Jurassic Tabbowa Basin in the northern part of study area could subside deeper than the Jurassic Andigama Basin in the southern part and/or deposition of reworking ancient OM in the Tabbowa fluvial system.

5.2. Origin of OM

The *n*-alkanes are commonly present in geological samples and are derived from certain biogenic sources (Eglinton and Hamilton, 1967; Meyers, 1997; Ratnayake et al., 2005; Jeng, 2006). The Andigama samples reveal that mixing of plankton/algae and microorganism (nC_{16}-C_{19}) and vascular plants (nC_{20}-C_{35}) (Fig. 2). The Andigama mudstones comprise a large proportion of middle-chain length *n*-alkanes (nC_{21}-C_{25}). Middle-chain length homologues are enhanced by bog-forming (swamp) vegetations (Ficken et al., 2000; Nott et al., 2000; Pancost et al., 2002; Bingham et al., 2010). In addition, TS values are very low (<0.001%) in the Andigama samples. Therefore, in our work, the Andigama mudstones can be interpreted as the development of freshwater lacustrine to swamp environments. The nC_{16}-C_{19} alkanes are less abundant in the sandy mudstone sample (Fig. 2(d)), possibly suggesting a lack of preservation in relatively high-energy depositional settings in the shallow burial depth estimated by the low maturity samples. On the other hand, the steranes in the Andigama samples are enriched in C_{29} and somewhat depleted in C_{28} and C_{27} (Fig. 9, Table 3). The C_{29} steranes are primarily derived from terrestrial higher plants (e.g., Meyers, 1997; Zhu et al., 2012), and C_{27} and C_{28} steranes are mainly derived from planktonic/algae in lacustrine and marine environments (Volkman, 2003; Piedad-Sánchez et al., 2004). The relative distributions of C_{27}-C_{28}-C_{29} steranes (Fig. 9) indicate that OMs in the Andigama sediments are mainly formed by the influx of land plant materials.

These results are also supported by the data of C/N ratio. C/N ratios have been extensively investigated to evaluate sources of bulk OM in sediments (e.g., Meyers and Ishiwatari, 1993; Meyers, 1997; Sampei and Matsumoto, 2001). Elevated C/N values of the Andigama mudstones (Table 2) indicate the large proportions of terrestrial OM. However, uncommonly low C/N ratio (2.9) of sandy mudstone (Table 2) should be interpreted as the effect of inorganic NH_4^+ absorbed by the clay (Müller, 1977). According to the effect of inorganic nitrogen, the C/N ratio becomes abnormally low in organic carbon poor sediments (Sampei and Matsumoto, 2001; Hossain et al., 2009).

As for the Tabbowa sandy sediments, *n*-alkanes compositions are dominated by lighter nC_{16}-C_{21} alkanes (Figs. 2(g-l)). The algae indicator ($<C_{20}/nC_{all}$ alkanes) implies that the Tabbowa beds are predominated by algal sources compared to the Andigama beds (Table 3). In addition, waxy long-chain *n*-alkanes (nC_{29}, nC_{31}, nC_{33}) of terrestrial OM are significantly deposited and preserved in all stratigraphic units in the Tabbowa beds (Figs. 2(g-l)). The C_{27}-C_{28}-C_{29} steranes also show that the Tabbowa sediments are mainly derived from aquatic organism with a significant amount of terrestrial higher plants (Figs. 2(g-l) and 9). The Aruwakkalu limestone and Red Earth are also abundant in algae OM. This does not conflict with C/N ratios as discussed above. The Tabbowa beds and the Miocene limestone record very low C/N values (Table 2).

Incidentally, the Ts/(Ts+Tm) ratios and CPI change according to both maturity and source variation (Waseda and Nishita, 1998; Inaba et al., 2001; Sawada, 2006). The Ts/(Ts+Tm) vs. sterane 20S/(20S+20R) ratios suggests that abundant input of terrestrial OM to shallow Andigama Basin and input of algae OM to deep Tabbowa Basin could occur respectively (Fig. 8(a)). Abundant low molecular *n*-alkanes ($<C_{20}$: Figs. 2(g-l)) with a significant higher *n*-alkanes ($>C_{29}$: Figs. 2(g-l)) and higher CPIs (Fig. 8(b)) in the Tabbowa Basin imply that nutrients for the production of algae OM could be from land area accompanied by terrestrial OM.

In contrast, aeolian transportation can act as a key process to deposit terrestrial OMs in the onshore sedimentary basins of the arid environments. In the present study, the highest CPI (Fig. 8(b)) and high ACL values in the Pleistocene Red Earth (Table 3) can probably indicate deposition of degraded ancient terrestrial OM (Jeng, 2006) under the prominent aeolian process. Specifically, the Red Earth paleosols at Aruwakkalu indicate intense biodegradation (Figs. 2(f) and 8(a)). As a result, some of the informative features of OM type may be lost.

5.3. Depositional environment

The TS are very low (less than the detection limit; <0.001%) even in the OM rich Andigama mudstone (Table 2). Low TS may suggest the freshwater or oxic seawater deposition (Berner, 1984; Berner and Raiswell, 1984). Such very low TS with high TOC can be interpreted as swamp/lake in the freshwater environment (Berner, 1984). The $C_{27}/(C_{27}+C_{29})$ 20R sterane vs. Pr/Ph ratios (2.1–3.0) of the Andigama sediments indicate that

the terrestrial OM was deposited under oxic conditions (Fig. 10).

The lower Pr/Ph values of the Tabbowa sediments (0.2–0.7, Fig. 10) may be affected by pelagic reducing conditions in algae/photosynthesis bacteria dominant sediments (Haven et al., 1987). Angular to sub-angular granitic sandy grains of the Tabbowa sediments can be reflected in the adjacent moderately low relief hinterland. The sedimentary facies with sandy grains and very low TS (%) distribution suggest fluvial freshwater deposition. Climate and depositional environment could influence the nature of the lithic fill in this succession, similar to the Jurassic Gondwana sediments of India (Dutta, 2002). The sequential sedimentary developments and correlation to the Indian Gondwana lithofacies (Facies C in Fig. 1(e)) can probably suggest warm semi-arid climate over geological time of the Tabbowa succession.

The slightly higher content of UCM in the Tabbowa beds (Figs. 2(g-l)) is possibly indicative of the relatively higher biodegradation compared to the Andigama samples. The UCM contents of the Aruwakkalu samples (Fig. 2(e) and 2(f)) are appreciably greater than those in the Jurassic sediments, indicating higher microbial activity.

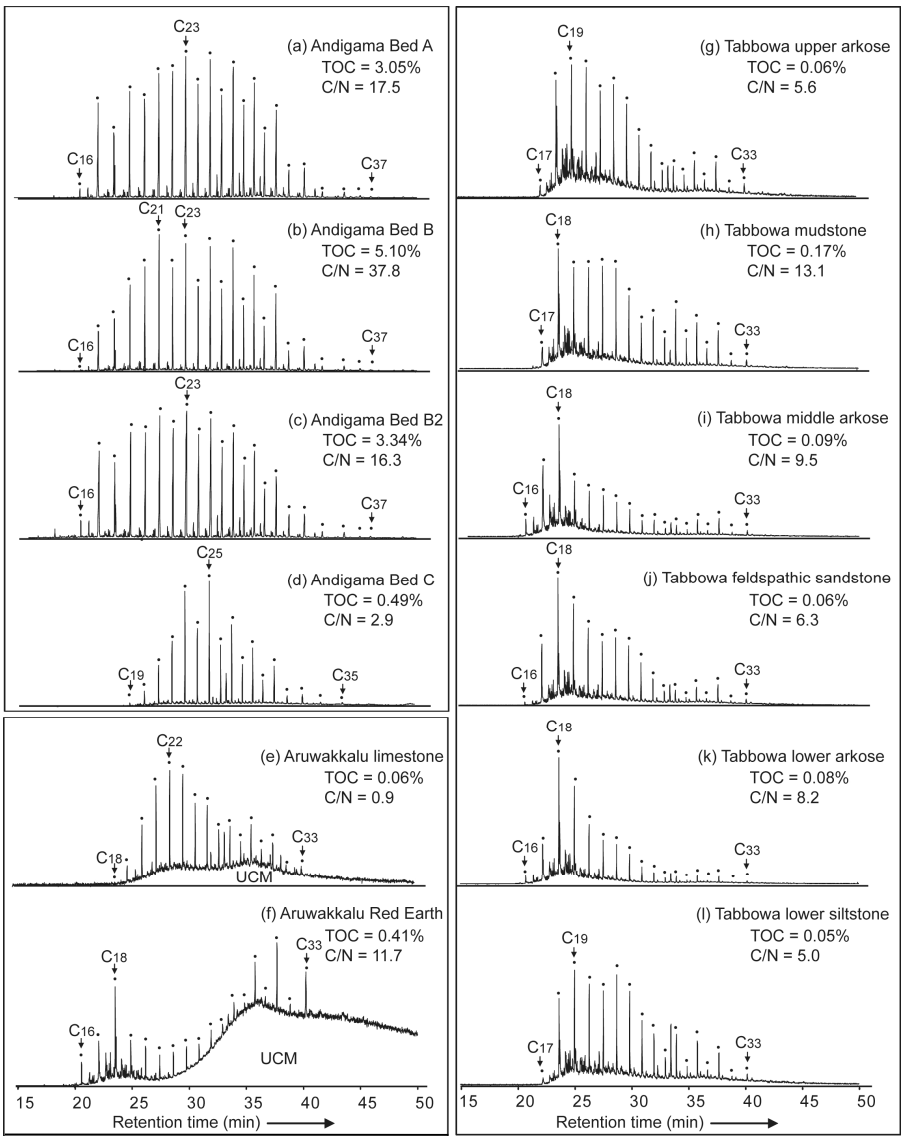

Fig. 2. Mass fragmentograms ($m/z=57$) showing distribution of *n*-alkanes in sediments of northwest onshore sedimentary units in Sri Lanka (UCM: unresolved complex mixture).

Table 4. Concentrations and ratios of PAHs in the Andigama mudstones.
b.d.l.: below detection limit, MPR: methylphenanthrene ratio, and MPI 3: methylphenanthrene index 3.
[a]Non-alkylated PAHs = (P + Fla + Py + BaAn + Chry + Tpn + Bflas + BePy + BaPy + Pery + InPy + BghiP + Cor)
[b]Alkylated PAHs = (Cad + Sim + Ret)
[c]MPR = [2-MP]/[1-MP]
[d]MPI 3 = ([2-MP] + [3-MP])/([1-MP] + [9-MP])

	Brown to black color Andigama mudstone		
	A	B	B2
Cad (μg/g TOC)	0.12	0.12	0.61
P (μg/g TOC)	0.17	0.14	0.44
Fla (μg/g TOC)	1.34	0.53	1.29
Py (μg/g TOC)	0.64	0.32	0.98
Sim (μg/g TOC)	4.49	3.44	3.82
Ret (μg/g TOC)	14.96	4.50	9.93
BaAn (μg/g TOC)	0.26	0.19	0.22
Chry + Tpn (μg/g TOC)	0.37	0.17	0.41
Bflas (μg/g TOC)	0.64	0.32	0.79
BePy (μg/g TOC)	0.29	0.18	0.36
BaPy (μg/g TOC)	0.20	0.13	0.26
Pery (μg/g TOC)	3.90	2.31	3.94
InPy (μg/g TOC)	0.07	0.05	0.08
BghiP (μg/g TOC)	0.26	0.16	0.29
Cor (μg/g TOC)	n.d.	n.d.	n.d.
Non-alkylated PAHs[a] (μg/g TOC)	8.13	4.51	9.07
Alkylated PAHs[b] (μg/g TOC)	19.56	8.07	14.36
Total PAHs (μg/g TOC)	27.69	12.57	23.43
MP/P	5.75	3.07	2.91
Fla/Py	2.09	1.68	1.31
Fla/(Fla + Py)	0.68	0.63	0.57
InPy/(InPy + Bpery)	0.29	0.33	0.30
BaAn/228	0.40	0.52	0.34
MPR[c]	0.30	0.41	0.40
MPI3[d]	0.35	0.48	0.45

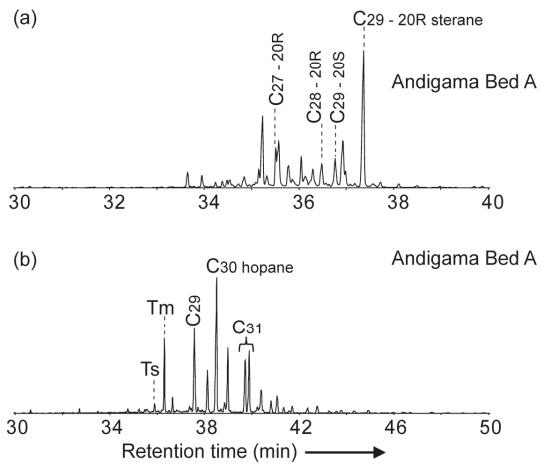

Fig. 3. Representative mass fragmentograms of (a) steranes (*m/z* = 217) and (b) pentacyclic triterpanes (*m/z* = 191).

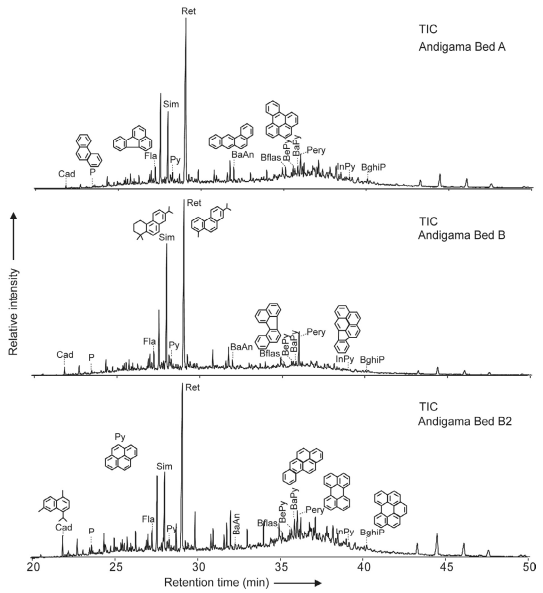

Fig. 4. Representation total iron chromatograms (TIC) of aromatic fraction showing distribution of PAHs in the Andigama mudstones.

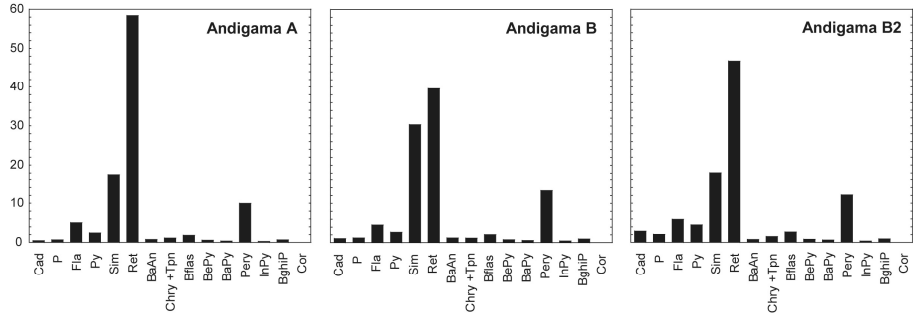

Fig. 5. Relative abundances of PAHs in the Andigama mudstones.

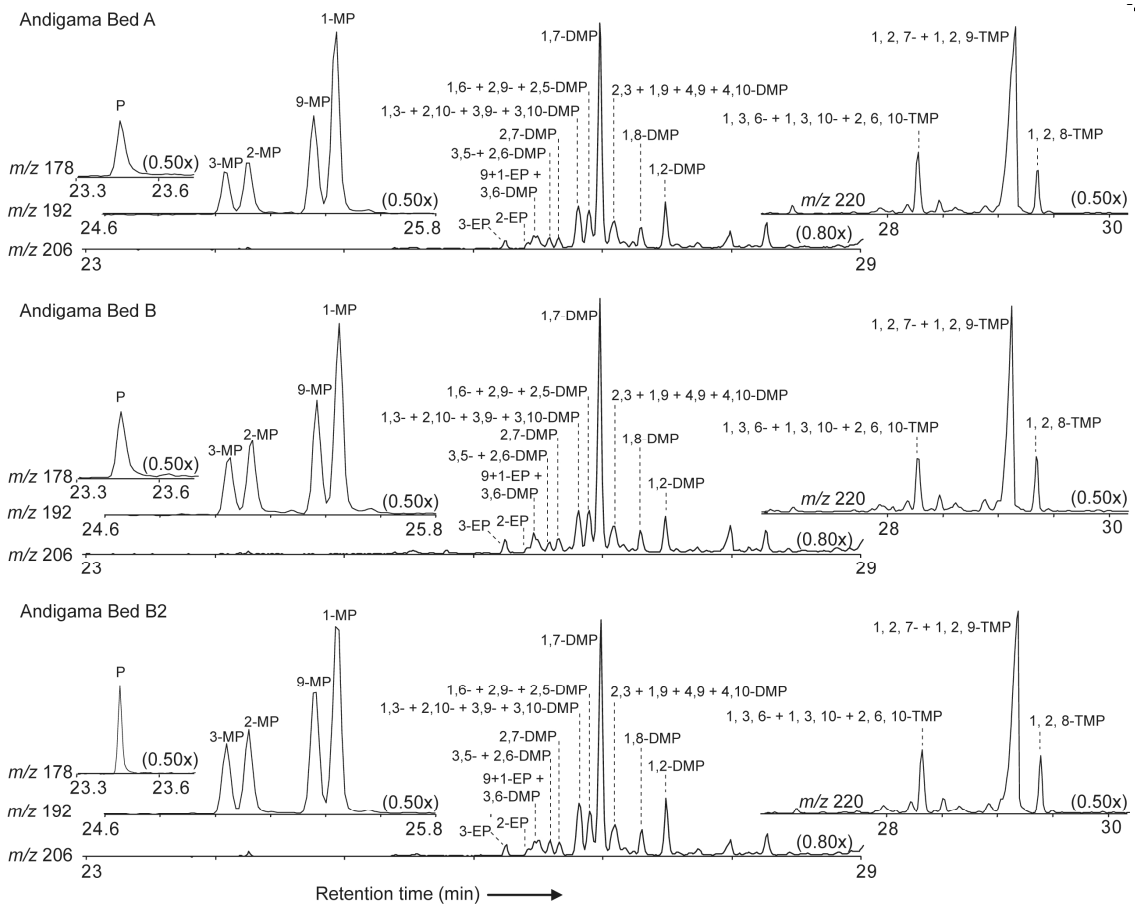

Fig. 6. Representative mass fragmentograms (*m/z* 178, 192, 206 and 220) for phenanthrene (P), methylphenanthrenes (MP), dimethylphenanthrenes (DMP) and trimethylphenanthrenes (TMP) in the Andigama mudstones.

5.4. PAHs distribution in the Andigama mudstones

The Andigama mudstones are dominated by Ret. Sim and Pery are secondarily/thirdly abundant, and minor peaks of Cad, P, Fla, Py, BaAn, Chry, Bflas, BePy, BaPy, InPy and BghiP can be observed (Figs. 4 and 5; Table 4). Ret is recognized as vascular plant marker represented by gymnosperm conifers (Jiang et al., 1998; Grice et al., 2007; Ei Mon Han et al., 2014). Sim is considered as main precursors of tri-aromatic Ret during diagenetic alteration (Yunker and Macdonald, 2003) and/or combustion of wood materials (Yunker et al., 2011). Therefore, these features imply that Ret and Sim

abundances in this basin (Figs. 4 and 5; Table 4) were controlled by gymnosperm OM such as conifer resins. In addition, Cad is another vascular plant marker that can be a diagenetic product of the cyclic sesquiterpenoidal hydrocarbons (Otto et al., 2002; Simoneit, 2005) and is detected in both angiosperm and gymnosperm coals for example in the Central Myanmar Basin (Ei Mon Han et al., 2014). However, the first unequivocal worldwide evidences of angiosperm records are from the Early Cretaceous (Friis et al., 2006). Also, oleanane type angiosperm biomarkers could not be detected in the analyzed samples suggesting that flowering plants had not yet evolved in the eastern Gondwanaland during the Jurassic (e.g., Aarssen et al., 2000). Therefore, in this study, low abundance of Cad compared to Ret and Sim can also be the indicator for gymnosperm plant resins.

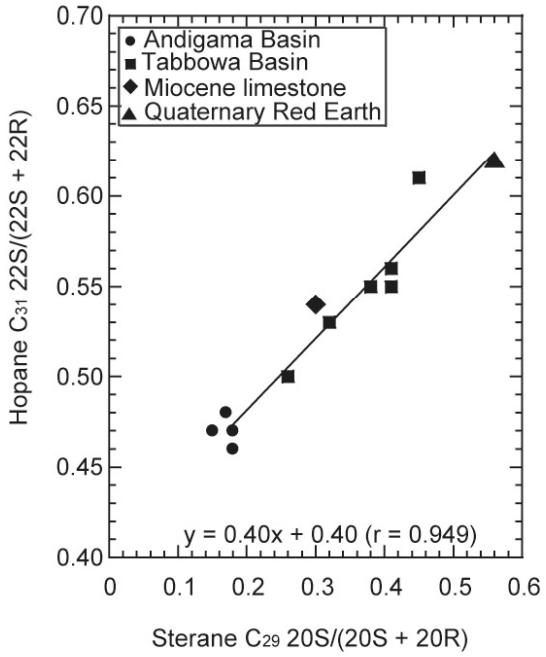

Fig. 7. Relationships between hopane C_{31} 22S/(22S+22R) and sterane C_{29} 20S/(20S+20R) ratios.

In contrast, Pery can be recognized as third abundance in non-alkylated PAHs from the Andigama Basin. Previous papers indicated that precursors of Pery can be fungi (Jiang et al., 2000), wood-degrading fungi (Suzuki et al., 2010; Marynowski et al., 2013), terrestrial sources (Stout and Emsbo-Mattingly, 2008) and depositional conditions (Silliman et al., 1998). A diagenetic product of Pery is predominantly observed in humid terrestrial OM rich (peat, coal and swamp) environments (Aizenshtat, 1973; Stout and Emsbo-Mattingly, 2008). Therefore, in this basin, Pery can be derived from wood-degrading fungi under the temperate humid climatic conditions.

The Andigama samples are also composed of a well-established combustion derive PAHs such as Fla, Py, BaAn, Chry+Tpn, Bflas, BePy, BaPy, InPy and BghiP (Figs. 4 and 5). The 5-ring BePy, InPy and BghiP PAHs can probably indicate high-temperature crown fire (O'Malley et al., 1997; Denis et al., 2012). Also, 4-ring Py, BaAn, Chry+Tpn and Bflas can probably indicate medium temperature ground fire (Jiang et al., 1998). According to Scott (2000), smaller living plants such as swamp vegetation, soil humus and peat provide fuel for the ground fire, whereas abundant productions of living trees provide fuel for activated wild fire. In the Andigama samples, the 4-ring PAHs are more abundant than the 5-ring ones (Fig. 5). Therefore, swamp vegetation and peat OM could be more abundant than trees OM in the Andigama Basin. The Tabbowa sediments, the Aruwakkalu limestone and Red Earth sediments did not contain such PAHs.

5.5. Alkylated phenanthrenes in the Andigama mudstones

Methylated aromatic isomers have been investigated in term of maturity parameters (Radke and Welte, 1983;

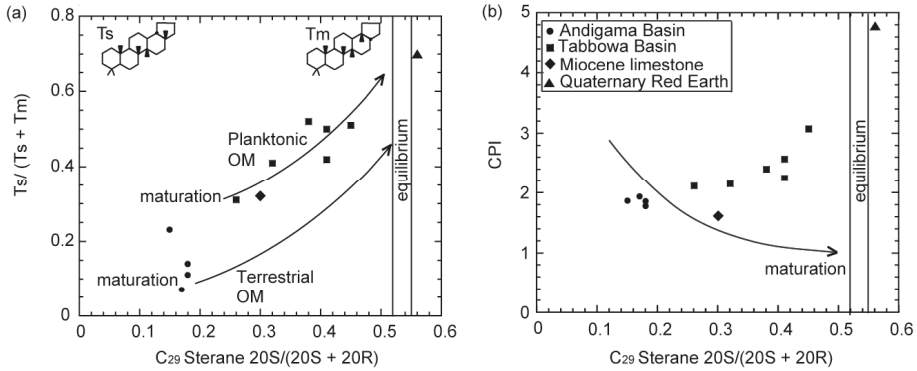

Fig. 8. (a) Ts/(Ts+Tm) ratio versus 20S/(20S+20R) of C_{29} sterane and (b) CPI versus 20S/(20S+20R) of C_{29} sterane for onshore sediments. Maturation trend lines (a) are from Waseda and Nishita (1998).

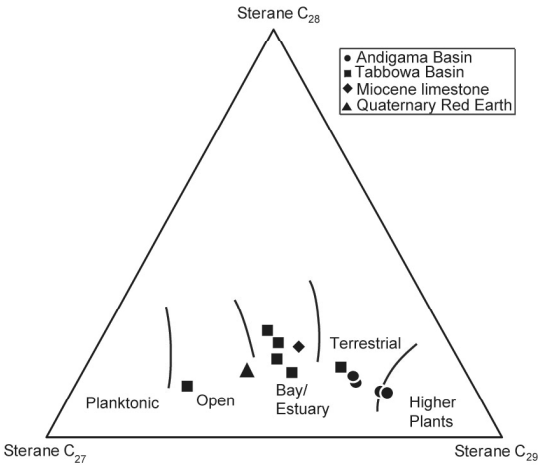

Fig. 9. Ternary diagram of C_{27}-C_{28}-C_{29} steranes showing OM sources and depositional environments (Huang and Meinschein, 1979).

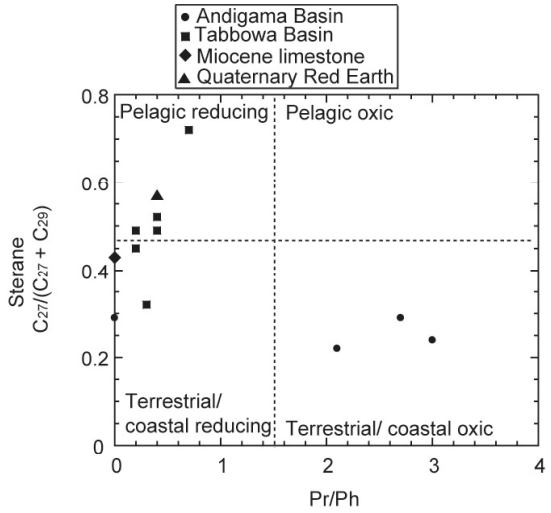

Fig. 10. Relationship between $C_{27}/(C_{27}+C_{29})$ sterane and Pr/Ph ratio showing OM sources and depositional conditions (Waseda and Nishita, 1998; Sawada, 2006).

Sampei et al., 1994; Chakhmakhchev and Suzuki, 1995), source indicators (Killops, 1991; Budzinski et al., 1995; Hossain et al., 2013) and secondary alteration processes such as biodegradation (Ahmed et al., 1999; Huang et al., 2004) of sedimentary rocks and petroleum. The MP mass fragments are characterized by predominant 1-MP with 9-MP isomers compared to 2-MP and 3-MP isomers (Fig. 6). 1-MP is originally predominant in terrestrial OM (Type-III kerogen) rich sediments (Budzinski et al., 1995; Maslen et al., 2011) and 9-MP is highly resistant to biodegradation (Ahmed et al., 1999; Huang et al., 2004). Further, Hossain et al. (2013) reported predominant 1-MP and 9-MP possibly originated from coniferous gymnosperm and pteridophyte plants in the Permian Gondwana coals and coaly shale in Bangladesh. In contrast, 2-MP and 3-MP are paramount in Type-I and Type-II kerogen respectively (Radke et al., 1986). Therefore, in this study, predominant 1MP isomer in the immature Andigama sediments can probably indicate less biodegraded gymnosperm OM.

Abundance of the 1, 7-DMP isomer is remarkably high compared to other DMP isomers (Fig. 6). The DMP is more resistant to biodegradation than P and the MP isomers (Huang et al., 2004). Armstroff et al. (2006) and Fabiańska et al. (2013) showed that 1, 7-DMP can be probably originated from the pimarane type diterpenoids due to decomposition of retene. Hossain et al. (2013) and Ei Mon Han et al. (2014) reported that the 1, 7-DMP was possibly originated from gymnosperm resin in Gondwana coal and coaly shale. This is consistent with the paleontological reports that gymnosperm/pteridophyte fossils were observed in the Jurassic mudstone and siltstone beds in Sri Lanka (Cooray, 1984; Edirisooriya and Dharmagunawardhane, 2013).

The relative abundances of 1, 2, 7-+1, 2, 9-TMP isomers are enhanced compared to the other TMP isomers (Fig. 6). The *αββ*-substituted 1, 3, 6-+1, 3, 10-+2, 6, 10-TMP, 1, 2, 7-+1, 2, 9-TMP and 1, 2, 8-TMP isomers can be identified as terrestrial markers in most of low maturity and less-biodegraded samples (Budzinski et al., 1995). Therefore, this high amount of 1, 2, 7-+1, 2, 9-TMP is also consistent with the terrestrial gymnosperm origin.

6. Conclusions

(1) Maturity of the Andigama mudstones are low in sterane C_{29} 20S/(20S+20R) (0.15–0.18) and the Tabbowa sediments are high (0.26–0.45). The Aruwakkalu limestone is 0.30 in sterane C_{29} 20S/(20S+20R), and Red Earth is mature about 0.56 probably due to over-matured OM from weathered metamorphic rocks. All sterane C_{29} 20S/(20S+20R) ratios (X) have an excellent correlation with the maturity parameter of hopane C_{31} 22S/(22S+22R) ratios (Y) (Y=0.40X+0.40, r=0.949, n=12), suggesting that sulfurized hopanoids were low abundance. The CPIs are mainly influenced by the contribution of reworked OM and not due to maturity in this study area.

(2) In the Jurassic Andigama Basin, a large proportion of middle-chain *n*-alkanes (nC_{21}-C_{25}), enriched C_{29} steranes and high C/N ratios (16.3–37.8) suggest swamp bog-forming origin. Very low TS (<0.001%) with high TOC (3.05–5.10%) and higher Pr/Ph ratios (2.1–3.0) suggest freshwater and oxic depositional environment. Abundant Ret, Sim and Pery indicate that the OM was influenced by gymnosperm with fungi in

the humid climatic conditions. Predominant 1-MP with 9-MP, 1, 7-DMP and 1, 2, 7-+1, 2, 9-TMP isomers probably indicate less biodegradable gymnosperm OM.

(3) The Jurassic Tabbowa Basin was filled by sandy sediments and TOC is very low (0.04–0.17%). The predominant nC_{16}-C_{21} alkanes with a minor peak of waxy *n*-alkanes (nC_{29}, nC_{31}, nC_{33}), abundant C_{27} steranes and higher Ts/(Ts+Tm) ratios suggest algal origin with a significant input of terrestrial OM. The fluvial sand grains and very low TS (<0.001%) distribution suggests lacustrine/fluvial freshwater deposition.

(4) The Miocene limestone shows very low TOC (0.06%) and algal origin. In the Pleistocene Aruwakkalu Red Earth, low TOC (0.41%), a high UCM, high CPI (4.78) and long ACL (29.9) can probably indicate oxidized and/or biodegraded ancient terrestrial OM during possible aeolian process.

Acknowledgement

This research was financially supported by a grant from MEXT Scholarship (the Japanese Ministry of Education and Culture) to the first author. We would like to thank Mr. C. W. Kularathne and Mr. C. Senevirathne for necessary field arrangements and guides. We gratefully acknowledge the valuable review comments of Dr. N. Takeda and Editor-in-Chief Dr. K. Sawada.

References

Aarssen B. G. K. V., Alexander R. and Kagi R. I. (2000) Higher plant biomarkers reflected palaeovegetation changes during Jurassic times. *Geochim. Cosmochim. Acta* **64**, 1417-1424.

Ahmed M., Smith J. W. and George S. C. (1999) Effects of biodegradation on Australian Permian coals. *Org. Geochem.* **30**, 1311-1322.

Aizenshtat Z. (1973) Perylene and its geochemical significance. *Geochim. Cosmochim. Acta* **37**, 559-567.

Armstroff A., Wilkes H., Schwarzbauer J., Littke R. and Horsfield B. (2006) Aromatic hydrocarbon biomarkers in terrestrial organic matter of Devonian to Permian age. *Palaeogeogr. Palaeoclimatol. Palaeoecol.* **240**, 253-274.

Berner R. A. (1984) Sedimentary pyrite formation: an update. *Geochim. Cosmochim. Acta* **48**, 605-615.

Berner R. A. and Raiswell R. (1984) C/S method for distinguishing freshwater from marine sedimentary rocks. *Geology* **12**, 365-368.

Bingham E. M., McClymont E. L., Väliranta M., Mauquoy D., Roberts Z., Chambers F. M., Pancost R. D. and Evershed R. P. (2010) Conservative composition of *n*-alkane biomarkers in *Sphagnum* species: implications for palaeoclimate reconstruction in ombrotrophic peat bogs. *Org. Geochem.* **41**, 214-220.

Budzinski H., Garrigues P. H., Connan J., Devillers J., Domine D., Radke M. and Oudin J. L. (1995) Alkylated phenanthrene distributions as maturity and origin indicators in crude oils and rock extracts. *Geochim. Cosmochim. Acta* **59**, 2043-2056.

Chakhmakhchev A. and Suzuki N. (1995) Aromatic sulfur compounds as maturity indicators for petroleum from the Buzuluk depression, Russia. *Org. Geochem.* **23**, 617-625.

Chatterjee S., Goswami A. and Scotese C. R. (2013) The longest voyage: Tectonic, magmatic, and paleoclimatic evolution of the Indian plate during its northward flight from Gondwana to Asia. *Gondwana Res.* **23**, 238-267.

Cooray P. G. (1984) An introduction to the Geology of Sri Lanka (2nd edn.). Ceylon National Museum Publication, Colombo.

Denis E. H., Toney J. L., Tarozo R., Anderson R. S., Roach L. D. and Huang Y. (2012) Polycyclic aromatic hydrocarbons (PAHs) in lake sediments record historic fire events: validation using HPLC-fluorescence detection. *Org. Geochem.* **45**, 7-17.

Dutta P. (2002) Gondwana lithostratigraphy of Peninsular India. *Gondwana Res.* **5**, 540-553.

Edirisooriya G. and Dharmagunawardhane H. A. (2013) Plant insect-interactions in Jurassic fossil flora from Sri Lanka. *Int. J. Sci. Res. Publ.* **3**, 1-13.

Eglinton G. and Hamilton R. J. (1967) Leaf epicuticular waxes. *Science* **156**, 1322-1335.

Ei Mon Han, Sampei Y. and Roser B. (2014) Upper Eocene coal and coaly shale in the Central Myanmar Basin: origin of organic matter and the effect of weathering. *Geochem. J.* **48**, 259-275.

Fabiańska M. J., Stanislaw R., Ćmiel S. R. and Misz-Kennan M. (2013) Biomarkers and aromatic hydrocarbons in bituminous coals of Upper Silesian Coal Basin: Example from 405 coal seam of the Zaleskie Beds (Poland). *Int. J. Coal Geol.* **107**, 96-111.

Farhaduzzaman Md., Abdullah W. H. and Islam Md. A. (2012) Depositional environment and hydrocarbon source potential of the Permian Gondwana coals from the Barapukuria Basin, Northwest Bangladesh. *Int. J. Coal Geol.* **90-91**, 162-179.

Farrimond P., Taylor A. and Telnaes N. (1998) Biomarker maturity parameters: the role of generation and thermal degradation. *Org. Geochem.* **29**, 1181-1197.

Ficken K. J., Li B., Swain D. L. and Eglinton G. (2000) An *n*-alkane proxy for the sedimentary input of submerged/floating freshwater aquatic macrophytes. *Org. Geochem.* **31**, 745-749.

Friis E. M., Pedersen K. R. and Crane P. R. (2006)

Cretaceous angiosperm flowers: Innovation and evolution in plant reproduction. *Palaeogeogr. Palaeoclimatol. Palaeoecol.* **232**, 251-293.

Grice K., Nabbefeld B. and Maslen E. (2007) Source and significance of selected polycyclic aromatic hydrocarbons in sediments (Hovea-3 well, Perth Basin, Western Australia) spanning the Permian-Triassic boundary. *Org. Geochem.* **38**, 1795-1803.

Haven H. L. T., Leeuw J. W. D., Rullkötter J. and Damsté J. S. S. (1987) Restricted utility of the pristane/phytane ratio as a palaeoenvironmental indicator. *Nature* **330**, 641-643.

Hossain H. M. Z., Sampei Y. and Roser B. P. (2009) Characterization of organic matter and depositional environment of Tertiary mudstones from the Sylhet Basin, Bangladesh. *Org. Geochem.* **40**, 743-754.

Hossain H. M. Z., Sampei Y., Hossain Q. H., Roser B. P. and Islam M. S. U. (2013) Characterization of alkyl phenanthrene distributions in Permian Gondwana coals and coaly shales from the Barapukuria Basin, NW Bangladesh. *Res. Org. Geochem.* **29**, 17-28.

Huang H., Bowler B. F. J., Oldenburg T. B. P. and Larter S. R. (2004) The effect of biodegradation on polycyclic aromatic hydrocarbons in reservoired oils from the Liaohe basin, NE China. *Org. Geochem.* **35**, 1619-1634.

Huang W. Y. and Meinschein W. G. (1979) Sterols as ecological indicators. *Geochim. Cosmochim. Acta* **43**, 739-745.

Inaba T., Suzuki N., Hirai A., Sekiguchi K. and Watanabe T. (2001) Source rock lithology prediction based on oil diacholestane abundance in the siliceous-clastic Akita sedimentary basin, Japan. *Org. Geochem.* **32**, 877-890.

Jeng W. L. (2006) Higher plant *n*-alkane average chain length as an indicator of petrogenic hydrocarbon contamination in marine sediments. *Mar. Chem.* **102**, 242-251.

Jiang C., Alexander R., Kagi R. I. and Murray A. P. (1998) Polycyclic aromatic hydrocarbons in ancient sediments and their relationships to palaeoclimate. *Org. Geochem.* **29**, 1721-1735.

Jiang C., Alexander R., Kagi R. I. and Murray A. P. (2000) Origin of perylene in ancient sediments and its geological significance. *Org. Geochem.* **31**, 1545-1559.

Katz M. B. (2000) Sri Lanka – India intraplate tectonics – Precambrian to Present. *Gondwana Res.* **3**, 3-5.

Killops S. D. (1991) Novel aromatic hydrocarbons of probable bacterial origin in a Jurassic lacustrine sequence. *Org. Geochem.* **17**, 25-36.

Köster J., van Kaam-Peters H. M. E., Koopmans M. P., de Leeuw J. W., Damsté J. S. S. (1997) Sulphurisation of homohopanoids: Effects on carbon number distribution, speciation and 22S/22R epimer ratios. *Geochim. Cosmochim. Acta* **61**, 2431-2452.

Marynowski L., Smolarek J., Bechtel A., Philippe M., Kurkiewicz S. and Simoneit B. R. T. (2013) Perylene as an indicator of conifer fossil wood degradation by wood-degrading fungi. *Org. Geochem.* **59**, 143-151.

Maslen E., Grice K., Métayer P. L., Dawson D. and Edwards D. (2011) Stable carbon isotopic compositions of individual aromatic hydrocarbons as source and age indicators in oils from western Australian basins. *Org. Geochem.* **42**, 387-398.

Meyers P. A. (1997) Organic geochemical proxies of paleooceanographic, paleolimnologic, and paleoclimatic processes. *Org. Geochem.* **27**, 213-250.

Meyers P. A. and Ishiwatari R. (1993) Lacustrine organic geochemistry–an overview of indicators of organic matter sources and diagenesis in lake sediments. *Org. Geochem.* **20**, 867-900.

Molnar P. and Tapponnier P. (1975) Cenozoic tectonics of Asia: effects of a continental collision. *Science* **189**, 419-426.

Müller P. J. (1977) C/N ratios in Pacific deep-sea sediments: Effect of inorganic ammonium and organic nitrogen compounds sorbed by clays. *Geochim. Cosmochim. Acta* **41,** 765-776.

Nott C. J., Xie S., Avsejs L. A., Maddy D., Chambers F. M. and Evershed R. P. (2000) *n*-Alkane distributions in ombrotrophic mires as indicators of vegetation change related to climatic variation. *Org. Geochem.* **31**, 231-235.

O'Malley V. P., Burke R. A. and Schlotzhauer W. S. (1997) Using GC-MS/Combustion/IRMS to determine the $^{13}C/^{12}C$ ratios of individual hydrocarbons produced from the combustion of biomass materials-application to biomass burning. *Org. Geochem.* **27**, 567-581.

Otto A., Simoneit B. R. T., Wilde V., Kunzmann L. and Püttmann W. (2002) Terpenoid composition of three fossil resins from Cretaceous and Tertiary conifers. *Rev. Palaeobot. Palynol.* **120**, 203-215.

Pan C., Peng D., Zhang M., Yu L., Sheng G. and Fu J. (2008) Distribution and isomerization of C_{31}-C_{35} homohopanes and C_{29} steranes in Oligocene saline lacustrine sediments from Qaidam Basin, Northwest China. *Org. Geochem.* **39**, 646-657.

Pancost R. D., Bass M., Geel B. V. and Damsté J. S. S. (2002) Biomarkers as proxies for plant inputs to peats: an example from a sub-boreal ombrotrophic bog. *Org. Geochem.* **33**, 675-690.

Piedad-Sánchez N., Suárez-Ruiz I., Martínez L., Izart A., Elie M. and Keravis D. (2004) Organic petrology and geochemistry of the Carboniferous coal seams from the Central Austrian Coal Basin (NW Spain). *Int. J. Coal Geol.* **57**, 211-242.

Radke M. and Welte D. H. (1983) The methylphenanthrene index (MPI): a maturity parameter based on

aromatic hydrocarbons. In: Bjorøy, M. et al. (eds.), *Advances in Organic Geochemistry* 1981. John Wiley and Sons, New York, pp. 504-512.

Radke M., Welte D. H. and Willsch H. (1986) Maturity parameters based on aromatic hydrocarbons: Influence of the organic matter type. In: Leythaeuser D., Rullkötter J. (Eds.), *Advances in Organic Geochemistry* 1985. John Wiley and Sons, New York, pp. 51-63.

Ratnayake A. S., Sampei Y. and Kularathne C. W. (2014) Stratigraphic responses to major depositional events from the late Cretaceous to Miocene in the Mannar Basin, Sri Lanka. *J. Geol. Soc. Sri Lanka* **16**, 5-18.

Ratnayake N. P., Suzuki N. and Matsubara M. (2005) Sources of long chain fatty acids in deep sea sediments from the Bering Sea and the North Pacific Ocean. *Org. Geochem.* **36**, 531-541.

Sampei Y. and Matsumoto E. (2001) C/N ratios in a sediment core from Nakaumi Lagoon, southwest Japan – usefulness as an organic source indicator –. *Geochem. J.* **35**, 189-205.

Sampei Y., Suzuki N., Mori K., Nakai T. and Sekiguchi K. (1994) Methylphenanthrenes from the MITI Takada-heiya well and thermally altered Kusanagi shales by dolerite intrusion in northeast Japan. *Geochem. J.* **28**, 317-331.

Sawada K. (2006) Organic facies and geochemical aspects in Neogene neritic sediments of the Takafu syncline area of central Japan: paleoenvironmental and sedimentological reconstructions. *Island Arc* **15**, 517-536.

Scott A. C. (2000) The Pre-Quaternary history of fire. *Palaeogeogr. Palaeoclimatol. Palaeoecol.* **164**, 297-345.

Silliman J. E., Meyers P. A. and Eadie B. J. (1998) Perylene: an indicator of alteration processes or precursor materials?. *Org. Geochem.* **29**, 1737-1744.

Simoneit B. R. T. (2005) A review of current applications of mass spectrometry for biomarker/molecular tracer elucidation. *Mass Spec. Rev.* **24**, 719-765.

Stout S. A. and Emsbo-Mattingly S. D. (2008) Concentration and character of PAHs and other hydrocarbons in coals of varying rank – implication for environmental studies of soils and sediments containing particular coal. *Org. Geochem.* **39**, 801-819.

Subroto E. A., Alexander R. and Kagi R. I. (1991) 30-Norhopanes: their occurrence in sediments and crude oils. *Chem. Geol.* **93**, 179-192.

Suzuki N., Yessalina S. and Kikuchi T. (2010) Probable fungal origin of perylene in Late Cretaceous to Paleogene terrestrial sedimentary rocks of north-eastern Japan as indicated from stable carbon isotopes. *Org. Geochem.* **41**, 234-241.

Tantrigoda D. A. and Geekiyanage P. (1991) An interpretation of gravity anomalies over the Andigama and Tabbowa sedimentary basins in north-west of Sri Lanka. *J. Natn. Sci. Coun. Sri Lanka* **19**, 39-51.

Volkman J. K. (2003) Sterols in microorganisms. *Appl. Microbiol. Biotechnol.* **60**, 495-506.

Waseda A. and Nishita H. (1998) Geochemical characteristics of terrigenous- and marine-sourced oils in Hokkaido, Japan. *Org. Geochem.* **28**, 27-41.

Yunker M. B. and Macdonald R. W. (2003) Alkane and PAH depositional history, sources and fluxes in sediments from the Fraser River Basin and Strait of Georgia, Canada. *Org. Geochem.* **34**, 1429-1454.

Yunker M. B., Lachmuth C. L., Cretney W. J., Fowler B. R., Dangerfield N., White L. and Ross P. S. (2011) Biota – sediments partitioning of aluminium smelter related PAHs and pulp mill related diterpenes by intertidal clams at Kitimat, British Columbia. *Mar. Environ. Res.* **72**, 105-126.

Zhu Y., Li Y., Zhou J. and Gu S. (2012) Geochemical characteristics of Tertiary coal-bearing source rocks in Xihu depression, East China Sea basin. *Mar. Petrol. Geol.* **35**, 154-165.